Photoluminescence and Spectroelectrochemistry of Single Ag Nanowires

Daniel A. Clayton,[†] Diane M. Benoist,[†] Yan Zhu,[†,‡] and Shanlin Pan[†,*]

[†]The University of Alabama, Department of Chemistry, Tuscaloosa, Alabama 35487-0336 and [‡]School of Chemical Engineering and Technology, Wuhan University of Technology, Wuhan, 430070, China

ABSTRACT We present strong photoluminescence from single Ag nanowires (NWs), their disordered blinking behavior, and their dependence on substrate potential. The stochastic bursts (<10 ms) in the photoluminescence trajectories of single Ag NWs in air are observed and attributed to the photoactivated fluorescence silver clusters. The dynamic changes in the photoluminescence are analyzed using autocorrelation function, statistical analysis of the stochastic durations, and probability density function to reveal the disordered nature of the spontaneous photochemical reaction at each individual Ag NWs under laser irradiation. Stable PL is observed for single Ag NWs in alkaline electrolyte and is found to be highly dependent on the electrochemical potential. The PL from single Ag NWs is found to be weakly dependent on polarization direction of the incident light and strongly dependent on the interactions with adjacent NWs.

KEYWORDS: nanowire · surface plasmon · SERS · photoluminescence · autocorrelation function · probability density

It is known that electronically excited silver nanostructures can emit photoluminescence (PL) under visible light irradiation.[1−7] Strong fluorescence is from excited Ag atoms, dimers, trimers, and other aggregation states of Ag atoms. Near-infrared[6] and visible[7] PL from silver nanowire (NW) arrays show broad emission spectrum under visible light excitation. Such interesting PL can be used to develop new optoelectronic devices and biosensors that can help unravel many mysteries underlying the complex characteristics of a biological system because silver clusters show strong, size dependent emission and are easy to make. Fluorescence silver clusters and nanoparticles have been prepared from silver oxide by photoactivation,[2] sputtering,[3] and encapsulation of silver clusters in a soft template (*e.g.*, cytosine oligonucleotide,[8] dendrimer,[9] and poly(acrylic acid))[10] by chemical reduction[9] or photoreduction methods.[11]

Silver NWs have interesting electrical and optical properties that can be used in a variety of applications[12] including transparent electrodes,[13,14] gas sensors,[15] biomolecular sensing,[16] photonic structures that can launch optical signals at a scale without optical refraction limits,[17,18] plasmonic antennae for surface-enhanced Raman scattering (SERS),[19−22] and fluorescence[23−25] of a dye molecule approximated to a Ag NW surface. Ag NWs are usually made by using template methods. The templates used for nanowire synthesis are usually made of hard materials, including porous alumina[26] and highly ordered pyrolytic graphite (HOPG)[27] and soft materials, such as polyvinylpyrrolidone (PVP),[28,29] cetyltrimethylammonium bromide (CTAB),[30] polysaccharide,[31] and DNA oligonucleotide.[32] Despite intense studies on their plasmonic activities for spectroscopic enhancement and synthetic work, there are few reports on the PL of single Ag NWs and their electrochemical characteristics. In addition, there are several important questions that need to be addressed to explore new applications of Ag NWs and understand their photochemical and electrochemical properties. Is the PL from a single Ag NW stable and excitation polarization dependent? How does one distinguish the PL from SERS of adsorbed species involved in the NW synthesis process? Is the PL dependent on the substrate electrochemical potential? Can one study single Ag electrochemical activities using the PL signal instead of collecting faradaic current from it? Furthermore, does the PL of Ag have uniform distribution along a single Ag NW?

In this report, we use combined optical and electrochemical methods[33,34] to investigate the PL of single Ag NWs. We present the PL and spectroelectrochemical activities of single silver nanowires through dynamic control of substrate potential in an alkaline electrolyte. PL from the nanowire is found

*Address correspondence to span1@bama.ua.edu.

Received for review January 18, 2010 and accepted March 18, 2010.

Published online March 31, 2010. 10.1021/nn100102k

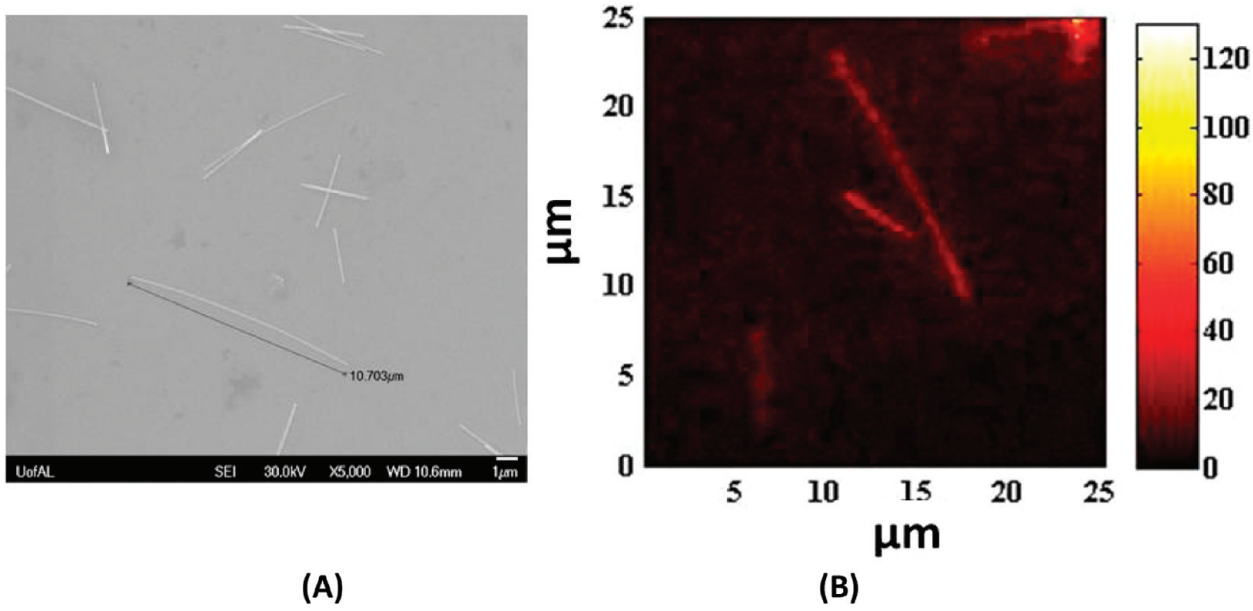

Figure 1. SEM image (A) of pristine silver nanowires; scanning fluorescence image of silver nanowires (B); 50 µW of 488 nm laser intensity was used; 10 msec collection time for each pixel.

to be highly dependent on excitation intensity and illumination time as well as electrode potential. Furthermore, Raman from adsorbed species on the Ag NWs can be seen in air but it is relatively weak compared to the PL from the silver nanowire. Single Ag NWs show stochastic changes in their PL trajectories. The disordered nature of PL emission due to a spontaneous photochemical reaction is discussed.

RESULTS AND DISCUSSION

Single Nanowire PL Imaging. Figure 1A shows a typical SEM image of silver nanowires on an ITO glass electrode. Silver nanowires have a diameter of about 90 nm and length of a few micrometers. The wires are well dispersed after being diluted with isopropanol and transferring onto ITO substrate. Such a wire-shaped nanostructure can be easily identified under a fluorescence/Raman microscope by simply imaging its one-dimentional structure. In addition, optical properties such as Raman enhancement and fluorescence are expected to be polarization dependent because the wire has both transverse plasmon bands and longitudinal plasmon bands at longer wavelengths. Finally, plasmonic coupling from adjacent sites on a single nanowire is expected to create hotspots along a single nanowire for surface enhanced photophysics. Figure 1B shows PL images of some silver nanowires under excitation of 488 nm with an excitation intensity of 50 µW. All nanowires show about a 500 nm width in the images instead of 90 nm due to the optical refraction limit. The dimensions of the wires in the fluorescence images are analogous to those obtained from the SEM results.

Time Evolution of PL Spectra of Single Ag NWs. Figure 2A shows another PL image of several Ag NWs with a better resolution than Figure 1B. Interestingly, the PL along the wire is not uniformly distributed along the wire-like SEM image shown in Figure 1A. This can be understood by the inhomogeneity in the crystal structure at different sites on the wire as well as the surface adsorption of surfactants such as polyvinylpyrrolidone that is used during the process of nanowire synthesis. In addition, stronger PL intensity can be observed at the point where the wires cross due to the coupling between the surface plasmons of two adjacent nanowires.[35] A typical PL spectrum of single Ag NW is shown in Figure 2B. The spectrum ranges from 595 to 650 nm and has a very sharp peak near 525 nm. The PL can be easily visualized under fluorescence microscope and shows dynamic fluctuation under intense laser irradiation. As shown in Figure 2C, dynamic changes of the PL can be revealed by the time evolution of the PL spectrum. Only 1 s per spectrum collection time was used to show the evolution of the spectrum due to the instrument response time limitation of our spectrometer and weak PL from single Ag NW.

Disordered Dynamic PL Blinking Behaviors of Single Ag NWs and Laser Intensity Dependences. To obtain a better time resolution to resolve the dynamic PL fluctuation of single Ag NW, we used an avalanche photodiode (APD) to collect PL through a confocal microscope. Figure 3 shows PL trajectory of one site on a single nanowire and statistic data, showing laser intensity dependent behavior of the PL of single silver nanowires. There is a minimum background signal when no silver nanowire is excited at 50 µW laser intensity. About 5000 photons per 10 ms are collected from the single site on the single nanowire with the same laser intensity. The zoom-in trajectory at this laser intensity is shown in Figure 4A. One of the interesting features of the data is

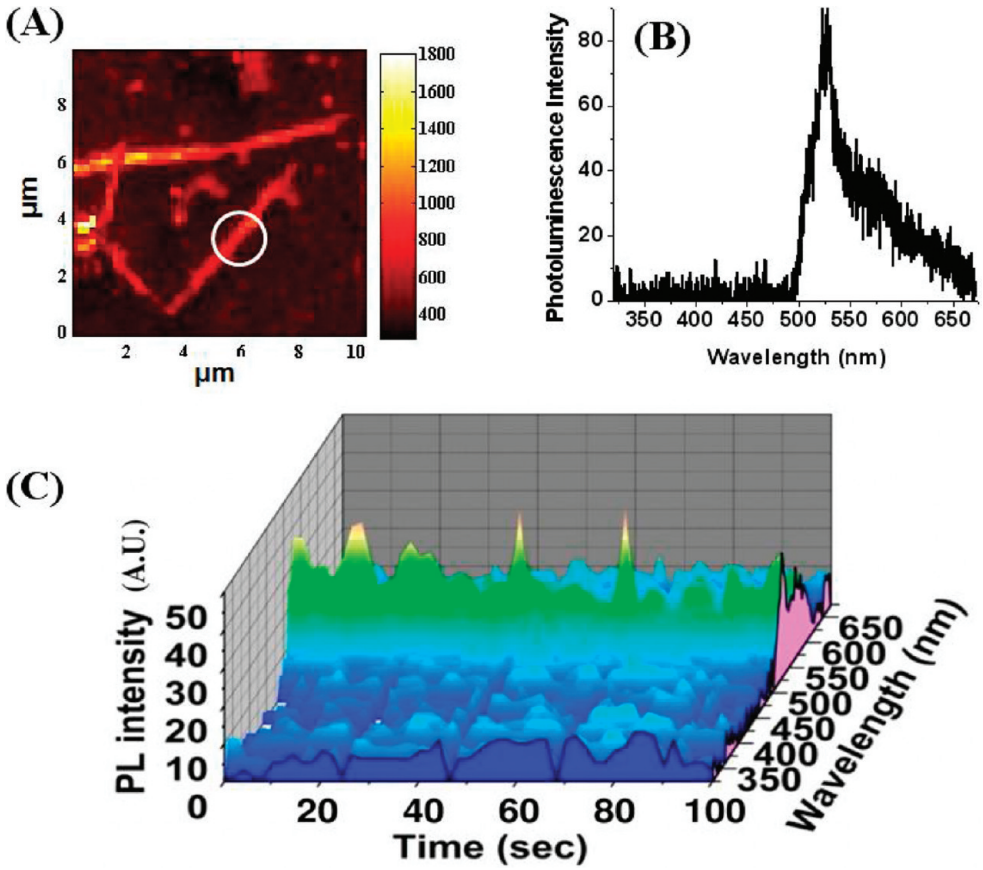

Figure 2. (A) Typical PL image of silver nanowires; (B) PL spectrum of a selected single silver, and (C) time evolution of the spectrum under continuous laser irradiation; 1 s collection time for each spectrum was used.

that there are highly frequent submillisecond bursts superimposed on the fluorescence baseline of the single silver nanowire. The frequency and height of the burst are highly dependent on the laser intensity and illumination time. Higher frequency and intensity bursts are obtained at longer illumination time and laser intensity. Such PL blinking behavior can also be observed from silver nanoparticles and could be attributed to random surface diffusion and subsequent agglomeration of Ag atoms leading to the formation of photoactive Ag nanoclusters.[36] Fluorescence of individual silver clusters can also be observed from photoactivated Ag_2O or partially oxidized silver film according to the results of Dickson and co-workers.[2] The photoactivated silver cluster can be excited by blue or green light sources to emit a wide range of photoluminescence from green to red. Similar results can be obtained from silver cluster on an AgBr surface according to Marchetti and co-

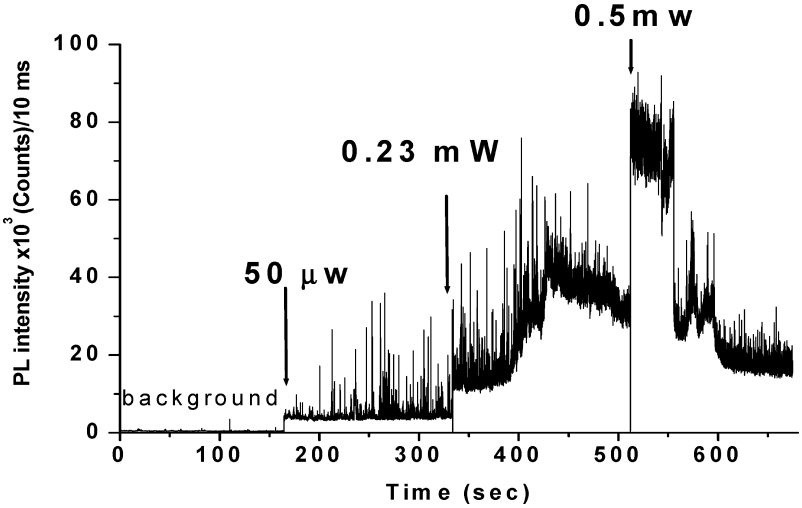

Figure 3. PL collected from a single silver nanowire in air. Laser intensity dependence of the PL collected per 10 ms. The single Ag NW is excited at 488 nm with laser intensity of 50 μW, 0.23 mW, and 0.5 mW, respectively.

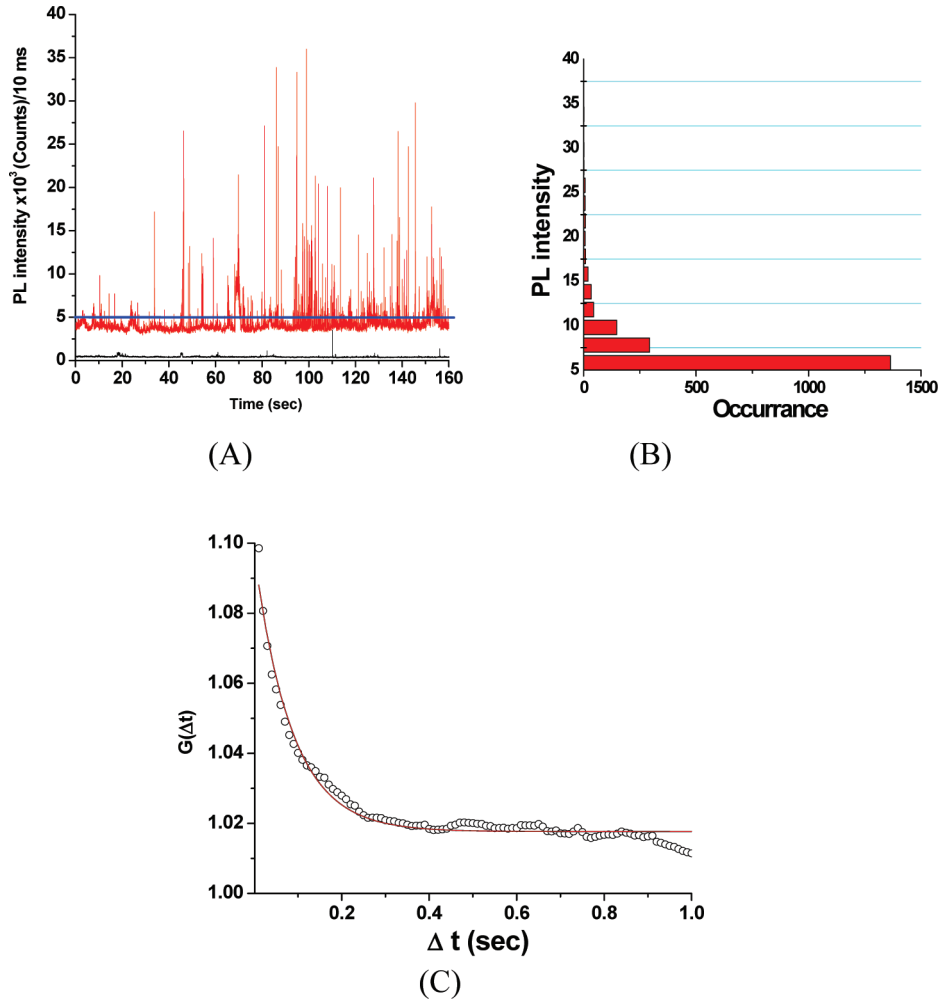

Figure 4. (A) Zoom-in PL intensity trajectory of a single nanowire under a laser intensity of 50 μW. (B) Statistic results of burst frequency of the data in B at certain peak height in counts and (C) temporal autocorrelation function $G(\Delta t)$.

workers.[37] These photoexcited states of silver clusters can emit light in ranges from 2.0 to 3.2 eV, depending on the size of the cluster and environment according to computational and experimental results.[1−3,37] In the case of photoluminescence blinking of Ag NWs, relationship between blinking frequency and photoluminescence burst height follows single exponential decay as shown by Figure 4C. The occurrences of weak blinking peaks dominate the occurrences histogram. When the single nanowire is excited at 0.5 mW, higher PL intensity is observed but decays quickly to a low level. This might be due to photochemical oxidation of silver and the formation of nonfluorescent large Ag aggregates under intense light irradiation. In addition, we also observed dramatic changes in emission color and intensity from individual emissive sites by using a fluorescence microscope. This can be explained by the changes in the Ag cluster size and charge that are constantly modified under illumination and chemical reaction.

It should also be noticed that the blinking behavior varies from one site to another under the same laser intensity. This can be understood by the nonuniform distribution of adsorbed organic molecules and silver oxides when the wires are dried and exposed to air. To test how the dynamic fluorescence activities behavior memorizes the initial state of light emission activities, we used the temporal autocorrelation function, $G(\Delta t)$, to estimate how the fluorescence intensity at time t =

TABLE 1. Calculated Decay Time Constant τ_{acs} from Temporal Autocorrelation Function, Power Exponents for ON States (m_{on}) and OFF States (m_{off}), Mean Value of Photoluminescence Intensity ($<I>$), Threshold Used for Occurrence Calculation ($I_{threshold}$), and the Maximum PL Intensity (I_{max}) in One Single Ag NW PL Trajectory

wire #	τ_{acs} (s)	m_{on}	m_{off}	$<I>$ cps	$I_{threshold}$	I_{max}
1	0.58	2.35	1.90	3108	3150	11000
2	0.08	2.20	1.78	4250	5000	36000
3	1.23	2.32	2.20	1347	1447	2680
4	2.19	2.66	1.60	2937	3070	9280
5	0.27	2.70	1.67	182	250	1616
6	0.53	2.40	2.08	1201	1245	8178
avg	0.81 (0.78)	2.44 (0.20)	1.87 (0.23)			

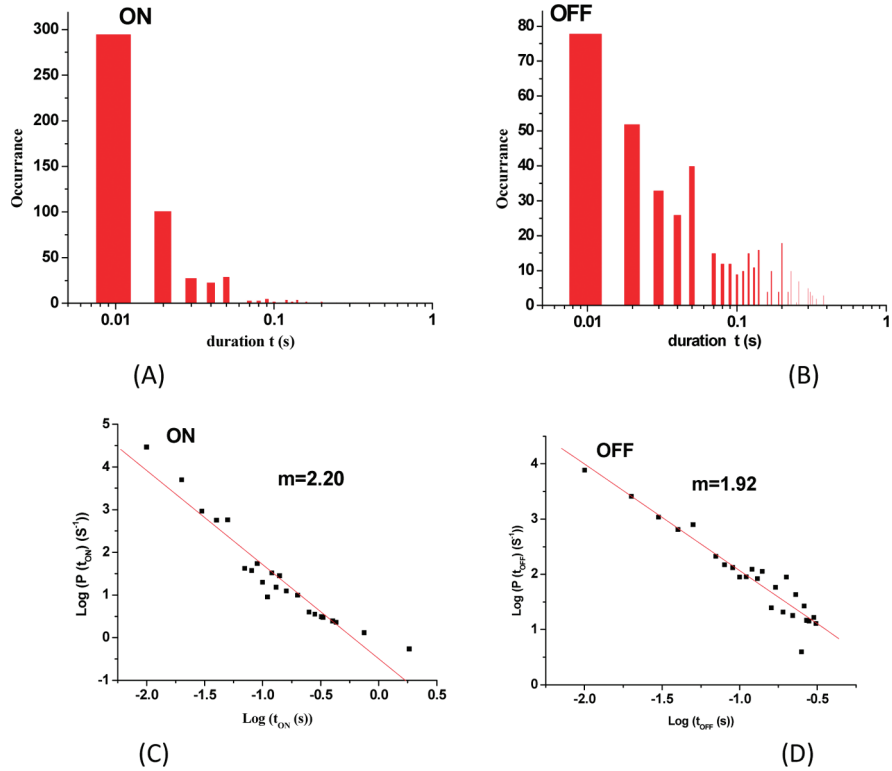

Figure 5. Distributions of occurrences of PL ON state (A) and OFF state (C) and corresponding probability density plots (B and D). The blinking trajectory used for the calculation is shown in Figure 4A. The solid blue line in Figure 4A indicates the PL intensity threshold used for the occurrences calculation.

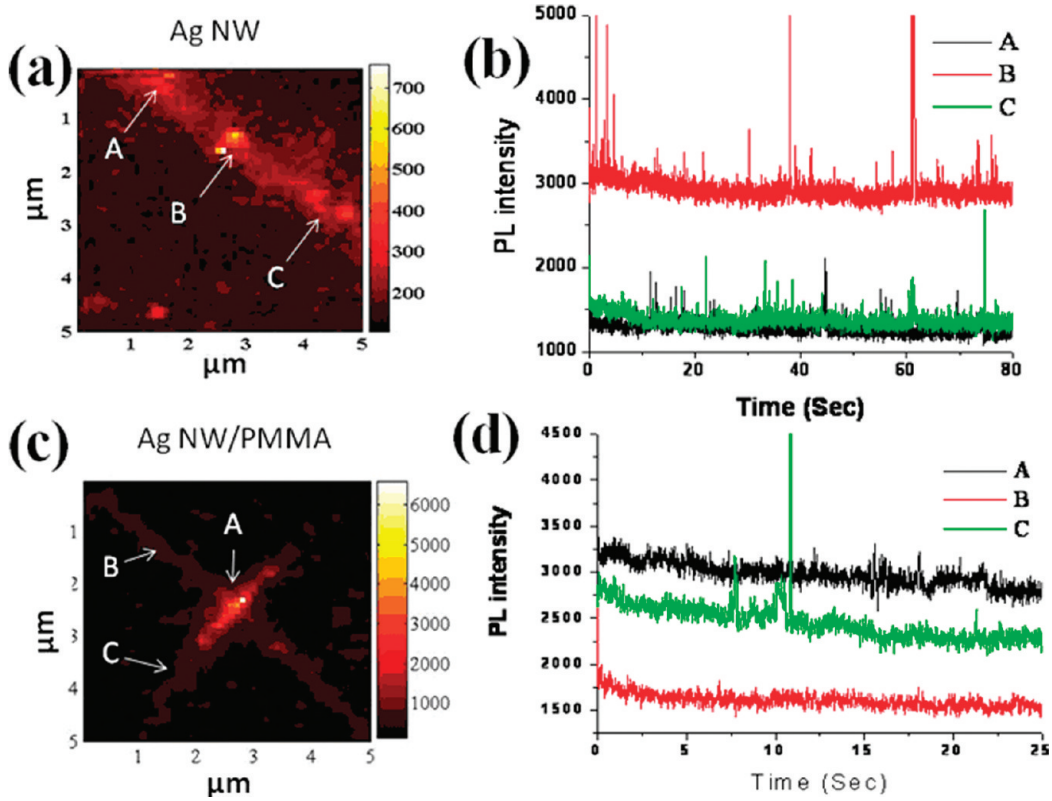

Figure 6. PL image (a) of single silver nanowire in air and (b) PL trajectories at three different sites on the wire excited with a laser intensity of 50 μW. Panel c shows typical PL image of two crossed Ag nanowires coated with PMMA. PL trajectories at three different sites on the wires excited with 50 μW of 532 nm laser intensity of are shown in panel d.

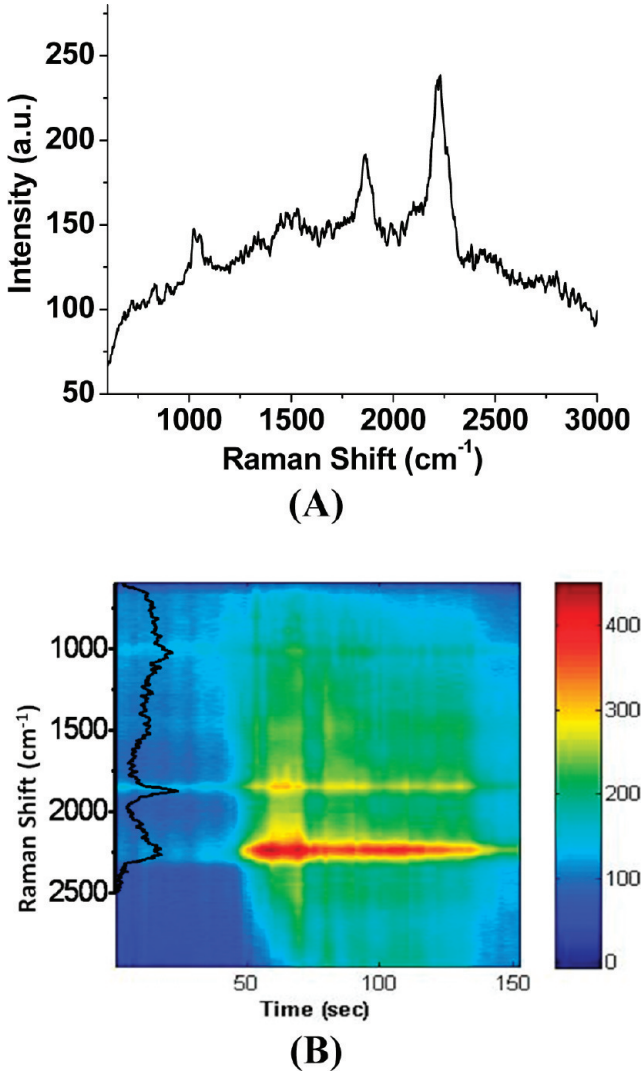

Figure 7. PL/Raman spectrum collected from a single silver nanowire in air (A) and time evolution of the spectrum (B) under continuous laser irradiation at 0.5 mW. 1 s collection time per spectrum is used.

0, $I(0)$, and the intensity at all times, t, later, $I(t)$, are correlated.

The autocorrelation function can be expressed as[38]

$$G(\Delta t) = \frac{\sum_{i=0}^{M-m} I(i\tau)I(i\tau + m\tau)}{\langle I\rangle^2(M - m)} \quad (1)$$

where m is an integer multiple of a time interval, τ, and $\Delta t = m\tau$ (where $0 \leq m < M$). $I(t)$ is the time-resolved fluorescence intensity with $M + 1$ data points ranging from $t = 0$ to $t = M\tau$. $\langle I\rangle$ is the mean PL intensity. As shown in Figure 4C, $G(\Delta t)$ shows a fast exponential decay with a short lifetime of about 80 ms, indicating that the loss of memory of initial state occurs due to a spontaneous photochemical reaction activities of Ag NWs. We collected PL blinking trajectories of several Ag NWs and analyzed their corresponding autocorrelation functions. An average decay time of about 0.81 ($\pm$0.78) second was obtained as listed in Table 1. Such spontaneous photochemical reaction at single Ag NW site can also be confirmed by performing statistical analysis on the stochastic durations and analyzing the probability density distribution of the ON and OFF states of single Ag NWs.

Figure 5A and B show the duration distributions of the ON and OFF states, respectively. The duration of OFF states spans ranges from a few milliseconds to seconds, while the one of ON states is shorter than 50 ms. The duration distributions of both ON and OFF states show no-Poisson behaviors because they show nonexponential decay. This phenomenon is similar to dynamic disorder fluctuation behavior of single molecule interfacial charge transfer activities.[39,40] To analyze such dynamic disordered blinking behavior, we constructed probability density distribution, $P(t) =$ occurrence $(t)/\Delta t$, for both ON and OFF states as shown in Figure 5C (ON) and D (OFF), respectively. The calculated probability density distributions show typical power-law behavior,[41,42] which can be mathematically described as $P(t)$ that is proportional to t^{-m}, m is a constant. We calculated m by constructing a linear fitting of the log−log plot of $P(t)$ and t^{-m}, as shown in Figure 5C and D for both ON and OFF states. The power exponents for six different Ag NWs are shown in Table 1. The value of m for ON states ranges from 2.20 to 2.70 and ranges from 1.60 to 2.20 for OFF state. The mean value $\langle m\rangle$ is 2.44 ($\pm$0.20) for ON states and 1.87 ($\pm$0.23) for OFF states, indicating that the disordered nature of the PL blinking behavior caused by photochemical reaction of silver in the presence of oxygen.

We then measured the photoluminescence trajectory of different sites of single Ag NWs in air and compared the dynamic PL changes with the PL of single nanowires coated with poly(methyl methacrylate) (PMMA). As shown in Figure 6a,b, we observed similar blinking behavior for single wires in air although three different sites of the wire show different blinking behavior due to the inhomogeneities in their crystal structures and surface modification. We found no stochastic blinking behavior for wires coated with PMMA (*cf.* Figure 6c,d). This indicates that the photochemical reaction of silver can be eliminated by surface polymer coating. We also tried the experiment in a nitrogen environment by purging the substrate using pure nitrogen. We observed dramatic decrease in both blinking frequency and fluorescence intensity of silver NWs. This further indicates the dynamic photochemical process involving oxygen from air.

Raman Spectra of Single Silver NWs. SERS of surfactant might also contribute to the blinking behavior because the temporally fluctuating (blinking) of a SERS signal can originate from several hot spots on a single Ag nanowire.[43,44] To probe the Raman information on the above-mentioned stochastic changes in the PL spectra, we collected the Raman spectrum from the single silver nanowires (Figure 7A) by using a high resolution grating. The Raman spectrum is found to be su-

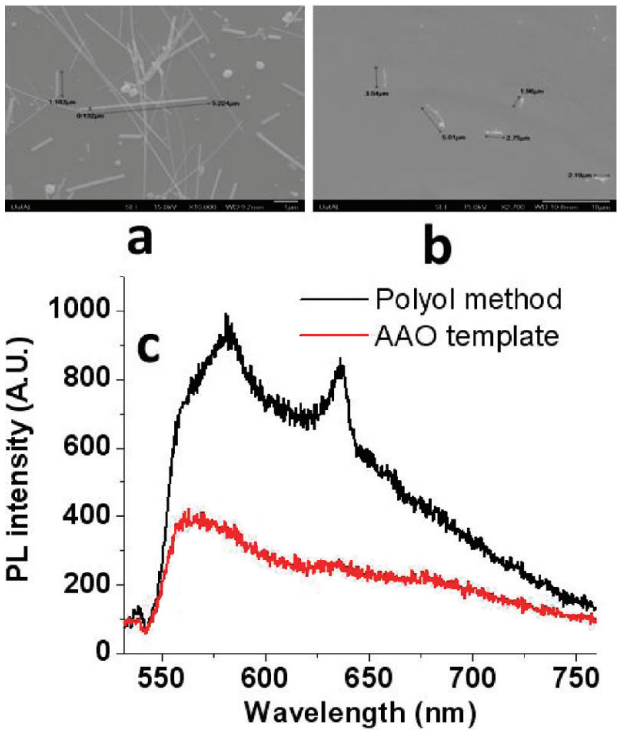

Figure 8. SEM images of silver nanowires prepared by polyol reduction method (a), AAO template method (b), and corresponding photoluminescence spectra of these two kinds of wires (c). Excitation wavelength: 532 nm.

perimposed onto a strong PL background of Ag. The Raman bands are supposed to come from species adsorbed by polyvinylpyrrolidone. By recording the evolution of the PL spectrum for one frame per second (*cf.* Figure 7B), we observed stochastic changes in both Raman and PL of silver under continuous excitation over 150 s. We expected to observe faster dynamic changes in the PL/Raman spectra, but our spectrum collection time cannot go down to the submillisecond. However, one should be convinced by the spectroscopic results that the bursts we observed should be from changes in PL of Ag not from Raman of adsorbed species as the PL of Ag dominates the spectrum.

PL of Ag NWs Made by Polyol Reduction Method and Porous Alumina Template Method. To confirm that the observed PL and blinking behaviors of single Ag nanowires are not typical results of *Seashell* Ag nanowires, we studied PL and blinking behavior of single Ag nanowires made by polyol reduction method and anodized alumina oxide (AAO) template methods. Figure 8 shows SEM images (a and b) and fluorescence spectra (c) of silver nanowires made by these two kinds of methods. Similar to *Seashell* silver nanowires, the PL of both polyol and AAO Ag nanowires can be easily visualized under a fluorescence microscope and shows dynamic fluctuation under intense laser irradiation. We then mapped the fluorescence of these two kinds of single Ag nanowires and studied their PL trajectories, and similar dynamic changes in PL intensity can be observed in air (*cf.* Figure 9).

Cyclic Voltammetry of Single Ag NWs. To further understand the dynamics in the photophysics of single Ag NWs, we studied the PL in aqueous solution and its dependence on the substrate potential, spectroelectrochemistry of single silver nanowires was measured. Figure 10A shows the schematic drawing of the setup for single Ag NW PL study. Cyclic voltammetry (CV) was performed while single nanowire PL intensity was recorded. The CV was run in the range of −0.15 and 0.45 V (vs Ag/AgCl) starting from 0.15 V in the positive direction to switch oxidation states of Ag NWs in the NaOH, while not to reduce the ITO. Figure 10B shows the effect of running the CV on the PL of a pristine silver nanowire sample. The current response is from all silver nanowires attached onto the ITO electrode, and includes no single nanowire information. It normally takes about twenty complete potential cycles before losing the oxidation and reduction features in the faradaic current peaks as seen around 0.28 V for the oxidation

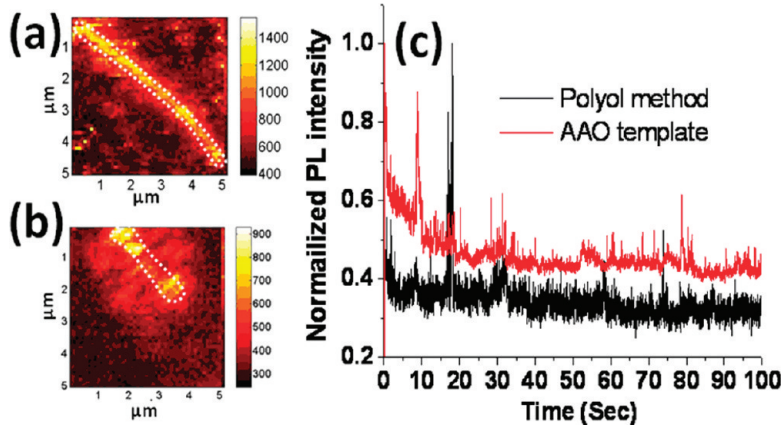

Figure 9. PL images of single Ag nanowires obtained by polyol reduction method (a), AAO template (b), and corresponding PL trajectories (c).

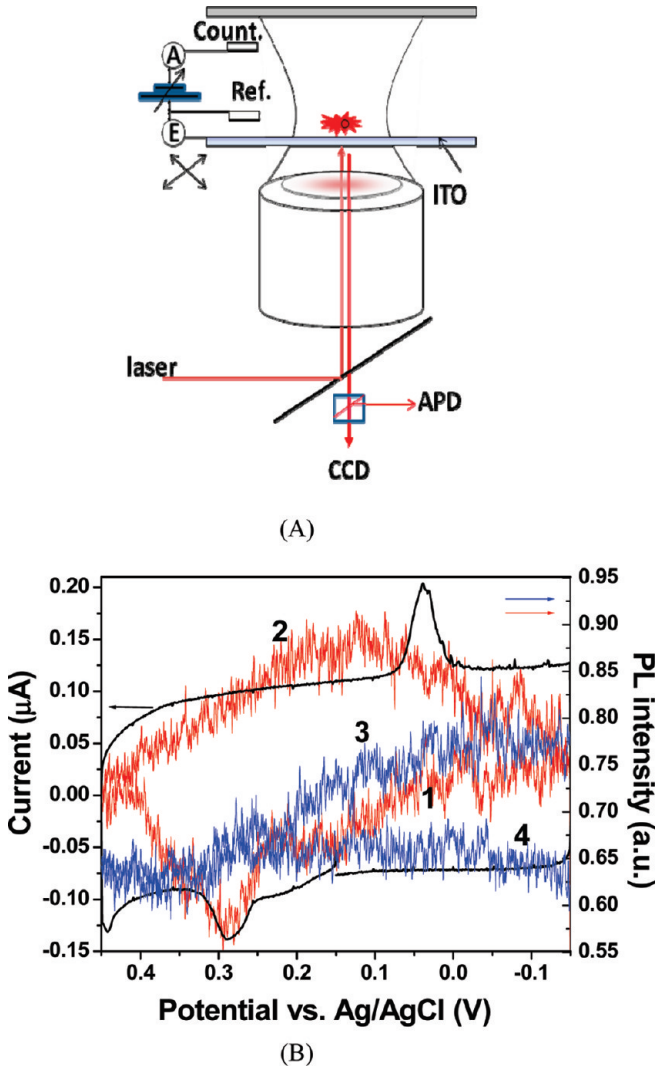

Figure 10. (A) Single nanowire spectroelectrochemistry setup comprised of a home-built confocal fluorescence microscope, a potentiostat and ultrasensitive photodetectors. (B) CV of silver nanowires and PL from single silver nanowires in 0.1 M NaOH. The red curve is the second complete cycle of the potential and the blue is the third cycle. The PL spectra of the first cycle are not shown. Scan rate: 0.01 V/sec. Reference electrode: Ag/AgCl.

reaction (Ag → Ag_2O) and 0.05 V for the reduction reaction (Ag_2O → Ag). We randomly selected one wire and measured its PL intensity while the CV was conducted, potential modulated PL can be observed as shown in the figure. The intensity of the PL is highly dependent on the substrate potential and also on the exposure time to the laser. We observed a dramatic increase in the PL intensity during the first potential cycle (not shown) because the wire was partially coated with silver oxide at rest potential in alkaline solution and the wire PL is activated under laser irradiation and negative overpotential. Starting from the second cycle of potential scan, the PL initially decreases when the electrode was scanned toward 0.45 V from −0.15 V and increases in the negative scan. The third cycle shows similar manner but the overall PL intensity decreases when the wire is illuminated using the laser. Compared to the results in air, no significant PL bursts show up in the PL trajectory in alkaline solution under potential control. This could be due to the fact that the fluorescent Ag clusters are deactivated when silver oxide overlay is formed in alkaline solution in comparison with Ag NWs in air. We then dried the oxidized silver NWs and photoactivated them under visible light leading to the recovery of the blinking behavior. This recovery of blinking behavior proves that the strong fluorescence silver clusters photoactivated are responsible for the blinking behavior of single Ag NWs in air.

We selected several nanowires and did similar measurements on their PL and dependence on applied potential scans. Some wires show pronounced PL dependence on the potential applied and relatively stable PL but others show PL decrease while reserving the potential dependence behavior. The different behavior from one wire to another might be due to their differences in their diameter, nature of electrical contact with ITO as well as charge transfer kinetics between ITO and silver. Overall, the PL intensity decreased upon surface oxidation but increased when the wire is reduced. This can be further confirmed by recording single Ag NW PL trajectory by applying a constant potential. As shown in Figure 11A, we show single Ag NW PL response when the substrate potential is stepped from 0 to 0.45 V and then back to 0 V. Similar to the results observed in Figure 10, PL is decreased when a fresh Ag NW gets oxidized at 0.45 V and increased at 0 V when the wire is reduced. We also studied the PL trajectory of oxidized and pristine silver nanowires under low power laser irradiation at open circuit potential. As shown in Figure 11B, the oxidized wire shows PL increase, indicating its silver oxide overlay easily decomposes under light and produces fluorescence silver at open circuit potential.

Polarization Angle Dependence of the PL of Ag NWs. We also investigated the polarization angle dependence of the PL of silver nanowires in both air and alkaline solution at open circuit potential. We first identified two individual Ag wires that crossed in a fairly perpendicular fashion. The typical area was then focused in on and scanned under polarized incident light. It appears that as polarization direction is rotated, that the intensity appears to change, with the vertical wire losing intensity as the horizontal wire gained intensity. Thus it can be assumed that silver nanowires exhibit some form of polarization dependence. When the wires are oxidized in alkaline solution, only discrete hot spots of PL can be observed and they show very weak polarization dependence. When the silver oxide layer is photoactivated by laser, silver clusters are made alongside the single nanowire to emit photoluminescence. In addition, very intense PL can be seen at the place where the two wires cross, due to the Plasmon coupling between the two wires. One application of this crossed point is for single molecule Raman when a tar-

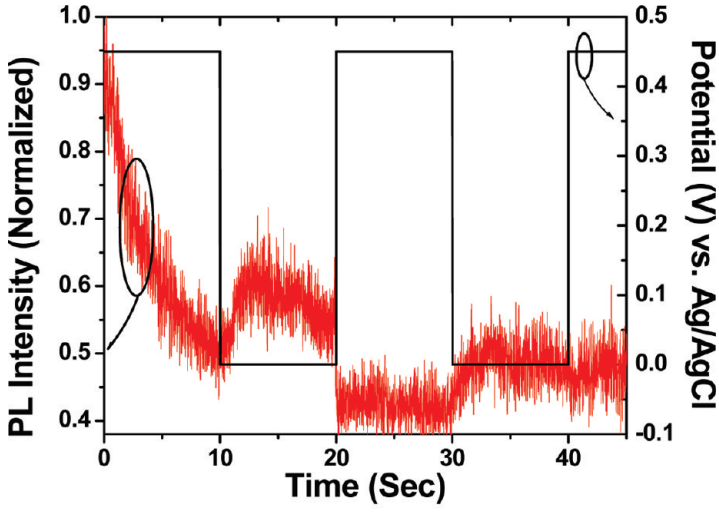

(A)

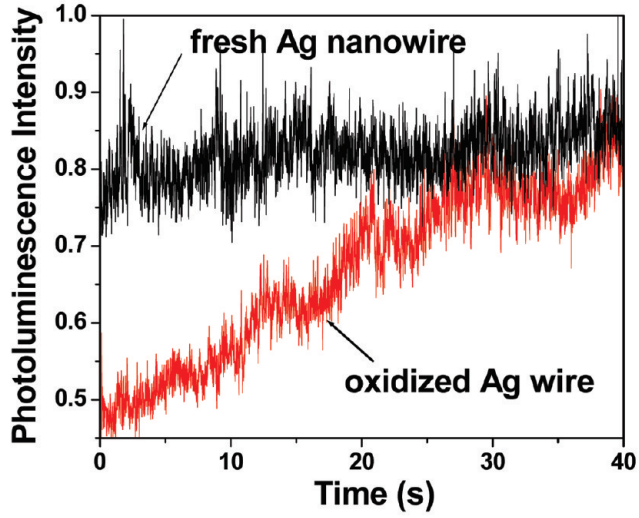

(B)

Figure 11. (A) Single Ag nanowire PL trajectories when a square potential wave is applied between 0.45 (vs Ag/AgCl) and 0.00 V in 0.1 M NaOH; (B) The PL trajectories of a fresh Ag nanowire and an oxidized Ag wire at open circuit potential in 0.1 M NaOH.

get molecule is precisely placed in the junction of two crossed Ag nanowires.

CONCLUSIONS

In summary, the stochastic changes in the PL of one site on a single nanowire in air can be attributed to the fluorescence photoactivated silver clusters not from Raman of adsorbed surfactant. This stochastic change in PL intensity of single silver nanowires can be explained by the disordered nature of a spontaneous photochemical reaction of silver. The PL of single silver nanowires in alkaline solution is highly dependent on the electrode potential and polarization direction of the incident light, providing a new way to study single Ag NW electrochemistry. Strong PL intensity can be obtained when two wires cross and are activated by laser irradiation at an open circuit potential. Our results can help understand the photoluminescence mechanism of silver nanostructures. The single Ag NW spectroelectrochemistry technique can be further extended to investigation the electrochemistry of single silver nanoparticle and other species involving silver clusters. Our technique can also be applied to studying interfacial charge transfer activities and catalytic reactions at the single nanoparticle level.

MATERIALS AND METHODS

All chemicals were used as received without further purification. NaOH and isopropanol were obtained from Fischer Scientific. Silver nanowires of a mean 89 nm diameter and 7.5 μm in length were obtained from Seashell Technology. The silver nanowires were diluted to a concentration of approximately 2

$\times 10^3$ nanowires per milliliter in isopropanol prior to use. A JEOL 7000 FE SEM was used to characterize nanowires.

Silver NW Made by Polyol Reduction Method.[45,46] Ethylene glycol (5 mL) was heated at ~160 °C with stirring in disposable glass vials placed in an oil bath. $CuCl_2 \cdot 2H_2O$/ethylene glycol solution (4 mM, 40 μL) was added, and the solution was allowed to heat for 15 min. A total of 1.5 mL of 114 mM (monomer concentration) polyvinylpyrrolidone (PVP)/ethylene glycol was then added, followed by 1.5 mL 94 mM $AgNO_3$/ethylene glycol. After about 10 min, the reaction was continued at ~160 °C without stirring and stopped when the solution became gray and wispy in an hour. The product was washed with acetone and water and finally stored in 2-propanol prior to use.

Ag NW Made by Using Alumina Template Method.[47] Anodized aluminum oxide (AAO; 1 cm (in diameter)) discs with 100 nm pores were purchased from Whatman. One side of the membrane was coated with solution-processed graphene oxide by using vacuum infiltration method to serve conductive substrate on one side of AAO template. The graphene oxide was synthesized from purified natural graphite (SP-1, Bay Carbon) by the Hummers method followed by hydrazine reduction.[48,49] Electrodeposition of silver rods into the pores was carried out by using a CHI 760C biopotentiostat (CHI, Austin, TX) with a platinum wire as counter electrode and Ag wire as quasi-reference electrode. Silver nanorods were grown into the oxide pores from 10 mM Ag_2SO_4 in 0.1 M Na_2SO_4 solution with the graphene oxide layer as working electrode. A 0.5 mA constant cathodic current was applied to the working electrode for 5 min while stirring the solution to form silver nanowires in the AAO template. After cleaning the fabricated template in an ultrasonic bath of DI water for 15 min to remove excess amorphous silver particles deposited on the surface of the AAO template and the graphene oxide backelectrode, the Ag infiltrated AAO template was dried and treated with 3 M NaOH for 5 min while shaking the solution to dissolve the aluminum oxide template completely. The released Ag NWs are washed with large amount of water and finally stored in 2-propanol prior to use.

Scanning Confocal Microscope. A Nano-View 200-2/M nanopositioner (Mad City Laboratories, Madison, WI) was mounted to the top of an Olympus IX-71 Inverted Microscope for scanning the nanowires. The sample was excited using a 488 nm self-contained argon-ion laser (Edmund Optics Inc.) and imaged with a ×100 numerical aperture oil-immersion objective (NA = 1.3). The emission was collected with the same objective and passed through a 488 nm laser filter set with long pass emission (Z488LP, Chroma Technology, Brattleboro, VT) and a 488 nm Rugate Notch Filter (Edmund Optics Inc.). The PL signal was then split, sending one part into a spectrometer with a liquid-nitrogen cooled digital CCD spectroscopy system (Acton Spec-10:100B, Princeton instruments, Trenton, NJ) through a monochromator (Acton SP-2558, Princeton instruments, Trenton, NJ) and the other to an avalanche photodiode (APD, SPEM-AQRH-15, PerkinElmer). PL from individual silver NWs can be collected at high efficiency with the laser turned off. A PC 6602 card from National Instruments Inc. was used for data acquisition. Date collection and control of the photon counter and nanopositioner were done using labview 8.5 (National Instruments Inc.). A camera (Q-Imaging, Olympus) was placed in the beam path after the filter but before the beam splitter to capture bright field images.

Electrochemical Cell for Spectroelectrochemistry. The electrochemical cell is placed on the microscope stage. The cell is made of Teflon, the bottom of which is open to accommodate a 0.17 mm slide (thermal fisher) coated with conductive transparent ITO layer (~100 nm) with a sheet resistance of 50 Ohms/sq (Metavac). The cell was mounted onto the nanopositioner and immobilized using edge clips. We used a hand-held Potentiostat (CHI1200A) for controlling the potential of the ITO substrate and a Pt wire and Ag/AgCl were used for counter and quasi-reference electrode (QRE), respectively. An ITO slide was glued to a FastWell (Grace BioLabs) by using 5 min epoxy (Thorlabs) then dry coated with the silver nanowire solution. After drying, the slide was rinsed with deionized water. The spacer was attached to the cell by using vacuum grease (Dow Corning) to prevent NaOH leakage. The cell was then with filled sodium hydroxide for *in situ* electrochemical and optical measurements.

Acknowledgment. This work is supported by the University of Alabama start-up funds. We acknowledge the University of Alabama Central Analytical Facility for their support of this work.

REFERENCES AND NOTES

1. König, L.; Rabin, I.; Schulze, W.; Ertl, G. Chemiluminescence in the Agglomeration of Metal Clusters. *Science* **1996**, *274*, 1353–1354.
2. Peyser, L. A.; Vinson, A. E.; Bartko, A. P.; Dickson, R. M. Photoactivated Fluorescence from Individual Silver Nanoclusters. *Science* **2001**, *291*, 103–106.
3. Harbich, W.; Fedrigo, S.; Meyer, F.; Lindsay, D. M.; Lignieres, J.; Rivoal, J. C.; Kreisle, D. Deposition of Mass Selected Silver Clusters in Rare Gas Matrixes. *J. Chem. Phys.* **1990**, *93*, 8535–8543.
4. Fedrigo, S.; Harbich, W.; Buttet, J. Optical Response of Silver Dimer, Silver Trimer, Gold Dimer, and Gold Trimer In Argon Matrixes. *J. Chem. Phys.* **1993**, *99*, 5712–17.
5. Felix, C.; Sieber, C.; Harbich, W.; Buttet, J.; Rabin, I.; Schulze, W.; Ertl, G. Fluorescence and Excitation Spectra of Ag4 in An Argon Matrix. *Chem. Phys. Lett.* **1999**, *313*, 105–109.
6. Gong, H. M.; Zhou, Z. K.; Xiao, S.; Su, X. R.; Wang, Q. Q. Strong Near-Infrared Avalanche Photoluminescence from Ag Nanowire Arrays. *Plasmonics* **2008**, *3*, 59–64.
7. Adhyapak, P. V.; Karandikar, P.; Vijayamohanan, K.; Athawale, A. A.; Chandwadkar, A. J. Synthesis of Silver Nanowires Inside Mesoporous MCM-41 Host. *Mater. Lett.* **2004**, *58*, 1168–1171.
8. Ritchie, C. M.; Johnsen, K. R.; Kiser, J. R.; Antoku, Y.; Dickson, R. M.; Petty, J. T. Ag Nanocluster Formation Using a Cytosine Oligonucleotide Template. *J. Phys. Chem. C* **2007**, *111*, 175–181.
9. Zheng, J.; Dickson, R. M. Individual Water-Soluble Dendrimer-Encapsulated Silver Nanodot Fluorescence. *J. Am. Chem. Soc.* **2002**, *124*, 13982–13983.
10. Yu, J.; Choi, S.; Dickson, R. M. Shuttle-Based Fluorogenic Silver-Cluster Biolabels. *Angew. Chem., Int. Ed.* **2009**, *48*, 318–320.
11. Zheng, J.; Ding, Y.; Tian, B.; Wang, Z. L.; Zhuang, X. Luminescent and Raman Active Silver Nanoparticles With Polycrystalline Structure. *J. Am. Chem. Soc.* **2008**, *130*, 10472–10473.
12. Zhang, Q.; Li, Y.; Xu, D.; Gu, Z. Preparation of Silver Nanowire Arrays In Anodic Aluminum Oxide Templates. *J. Mater. Sci. Lett.* **2001**, *20*, 925–927.
13. De, S.; Higgins, T. M.; Lyons, P. E.; Doherty, E. M.; Nirmalraj, P. N.; Blau, W. J.; Boland, J. J.; Coleman, J. N. Silver Nanowire Networks As Flexible, Transparent Conducting Films: Extremely High DC To Optical Conductivity Ratios. *ACS Nano* **2009**, *3*, 1767–1774.
14. Lee, J.; Connor, S. T.; Cui, Y.; Peumans, P. Solution-Processed Metal Nanowire Mesh Transparent Electrodes. *Nano Lett.* **2008**, *8*, 689–692.
15. Murray, B. J.; Li, Q.; Newberg, J. T.; Hemminger, J. C.; Penner, R. M. Silver Oxide Microwires: Electrodeposition and Observation of Reversible Resistance Modulation upon Exposure to Ammonia Vapor. *Chem. Mater.* **2005**, *17*, 6611–6618.
16. Brunker, S. E.; Cederquist, K. B.; Keating, C. D. Metallic Barcodes for Multiplexed Bioassays. *Nanomedicine* **2007**, *2*, 695–710.
17. Pyayt, A. L.; Wiley, B.; Xia, Y.; Chen, A.; Dalton, L. Integration Of Photonic and Silver Nanowire Plasmonic Waveguides. *Nat. Nanotechnol.* **2008**, *3*, 660–665.
18. Fang, Y.; Wei, H.; Hao, F.; Nordlander, P.; Xu, H. Remote-Excitation Surface-Enhanced Raman Scattering Using Propagating Ag Nanowire Plasmons. *Nano Lett.* **2009**, *9*, 2049–2053.
19. Baik, J. M.; Lee, S. J.; Moskovits, M. Polarized Surface-Enhanced Raman Spectroscopy from Molecules Adsorbed in Nano-Gaps Produced by Electromigration in Silver Nanowires. *Nano Lett.* **2009**, *9*, 672–676.
20. Fang, Y.; Wei, H.; Hao, F.; Nordlander, P.; Xu, H. Remote-Excitation Surface-Enhanced Raman Scattering Using

Propagating Ag Nanowire Plasmons. *Nano Lett.* **2009**, *9*, 2049–2053.
21. Yoon, I.; Kang, T.; Choi, W.; Kim, J.; Yoo, Y.; Joo, S.; Park, Q.; Ihee, H.; Kim, B. Single Nanowire on a Film as an Efficient SERS-Active Platform. *J. Am. Chem. Soc.* **2009**, *131*, 758–762.
22. Mohanty, P.; Yoon, I.; Kang, T.; Seo, K.; Varadwaj, K. S. K.; Choi, W.; Park, Q.; Ahn, J. P.; Suh, Y. D.; Ihee, H.; Kim, B. Simple Vapor -Phase Synthesis of Single-Crystalline Ag Nanowires and Single- Nanowire Surface-Enhanced Raman Scattering. *J. Am. Chem. Soc.* **2007**, *129*, 9576–9577.
23. Guo, S.; Britti, D. G.; Heetderks, J. J.; Kan, H.; Phaneuf, R. J. Spacer Layer Effect in Fluorescence Enhancement from Silver Nanowires over a Silver Film; Switching of Optimum Polarization. *Nano Lett.* **2009**, *9*, 2666–2670.
24. Pan, S.; Wang, Z.; Rothberg, L. J. Enhancement of Adsorbed Dye Monolayer Fluorescence by a Silver Nanoparticle Overlayer. *J. Phys. Chem. B* **2006**, *110*, 17383–17387.
25. Pan, S.; Rothberg, L. J. Enhancement of Platinum Octaethyl Porphyrin Phosphorescence near Nanotextured Silver Surfaces. *J. Am. Chem. Soc.* **2005**, *127*, 6087–6094.
26. Zong, R.; Zhou, J.; Li, Q.; Du, B.; Li, B.; Fu, M.; Qi, X.; Li, L.; Buddhudu, S. Nanowire Arrays Embedded in Anodic Alumina Membrane. *J. Phys. Chem. B* **2004**, *108*, 16713–16716.
27. Walter, E. C.; Murray, B. J.; Favier, F.; Kaltenpoth, G.; Grunze, M.; Penner, R. M. Noble and Coinage Metal Nanowires by Electrochemical Step Edge Decoration. *J. Phys. Chem. B* **2002**, *106*, 11407–11411.
28. Sun, Y.; Gates, B.; Mayers, B.; Xia, Y. Crystalline Silver Nanowires by Soft Solution Processing. *Nano Lett.* **2002**, *2*, 165–168.
29. Wiley, B.; Sun, Y.; Xia, Y. Synthesis of Silver Nanostructures with Controlled Shapes and Properties. *Acc. Chem. Res.* **2007**, *40*, 1067–76.
30. Jana, N. R.; Gearheart, L.; Murphy, C. J. Wet Chemical Synthesis of Silver Nanorods and Nanowires of Controllable Aspect Ratio. *Chem. Commun.* **2001**, *7*, 617–618.
31. Kong, J.; Ferhan, A. R.; Chen, X.; Zhang, L.; Balasubramanian, N. Polysaccharide Templated Silver Nanowire for Ultrasensitive Electrical Detection of Nucleic Acids. *Anal. Chem.* **2008**, *80*, 7213–7217.
32. Fischler, M.; Simon, U.; Nir, H.; Eichen, Y.; Burley, G. A.; Gierlich, J.; Gramlich; Philipp, M. E.; Carell, T. Formation of Bimetallic Ag-Au Nanowires by Metallization of Artificial DNA Duplexes. *Small* **2007**, *3*, 1049–1055.
33. Benoist, D.; Pan, S. L. Activation of TiO_2 Electrode Using Gold Particles for Efficient Electrogenerated-Chemiluminescence (ECL) from Ruthenium Complex in Aqueous Solution. *J. Phys. Chem. C* **2010**, *114*, 1815–1821.
34. Pan, S. L., Wang, G. L. Single-molecule and single-nanoparticle electrochemistry at nanoelectrodes and spectroelectrochemistry. In *Trace Analysis with Nanomaterials*, Pierce, D., Ed.; Wiley-VCH: New York, 2009.
35. Brus, L. Noble Metal Nanocrystals: Plasmon Electron Transfer Photochemistry and Single-Molecule Raman Spectroscopy. *Acc. Chem. Res.* **2008**, *41*, 1742–1749.
36. Wu, X.; Yeow, E. K. L. Fluorescence Blinking Dynamics of Silver Nanoparticle and Silver Nanorod Films. *Nanotechnology* **2008**, *19*, 035706/1–035706/6.
37. Marchetti, A. P.; Muenter, A. A.; Baetzold, R. C.; McCleary, R. T. Formation and Spectroscopic Manifestation of Silver Clusters on Silver Bromide Surfaces. *J. Phys. Chem. B* **1998**, *102*, 5287–5297.
38. Wang, Z. J.; Rothberg, L. J. Structure and Dynamics of Single Conjugated Polymer Chromophores by Surface-Enhanced Raman Spectroscopy. *ACS Nano* **2007**, *1*, 299–306.
39. Wang, Y. M.; Wang, X. F.; Lu, H. P. Probing Single-Molecule Interfacial Geminate Electron-Cation Recombination Dynamics. *J. Am. Chem. Soc.* **2009**, *131*, 9020–9025.
40. Lu, H P; Xun, L; Xie, X. S. Single-Molecule Enzymatic Dynamics. *Science* **1998**, *282*, 1877–1882.
41. Wang, Y. M.; Wang, X. F.; Ghosh, S. K.; Lu, H. P. Probing Single-Molecule Interfacial Electron Transfer Dynamics of Porphyrin on TiO_2 Nanoparticles. *J. Am. Chem. Soc.* **2009**, *131*, 1479–1487.
42. Kuno, M.; Fromm, D. P.; Hamann, H. F.; Gallagher, A.; Nesbitt, D. J. "On"/"Off" Fluorescence Intermittency of Single Semiconductor Quantum Dots. *J. Chem. Phys.* **2001**, *115*, 1028–1040.
43. Sladkova, M.; Vlckova, B.; Pavel, I.; Siskova, K.; Slouf, M. Surface-Enhanced Raman Scattering From a Single Molecularly Bridged Silver Nanoparticle Aggregate. *J. Mol. Struct.* **2009**, *924−926*, 567–570.
44. Ward, D. R.; Halas, N. J.; Ciszek, Jacob, W.; Tour, J. M.; Wu, Y.; Nordlander, P.; Natelson, D. Simultaneous Measurements of Electronic Conduction and Raman Response in Molecular Junctions. *Nano Lett.* **2008**, *8*, 919–924.
45. Xia, Y.; Yang, P.; Sun, Y.; Wu, Y.; Mayers, B.; Gates, B.; Yin, Y.; Kim, F.; Ya, H. One-Dimensional Nanostructures: Synthesis, Characterization, and Applications. *Adv. Mater.* **2003**, *15*, 353–389.
46. Korte, K. E.; Skrabalak, S. E.; Xia, Y. N. Rapid synthesis of Silver Nanowires Through a CuCl- or $CuCl_2$-Mediated Polyol Process. *Mater. Chem.* **2008**, *18*, 437–441.
47. Wang, Z. J.; Pan, S. L.; Krauss, T. D.; Du, H.; Rothberg, L. J. The Structural Basis for Giant Enhancement Enabling Single-Molecule Raman Scattering. *Proc. Nat. Acad. Sci. U.S.A.* **2003**, *100*, 8638–8643.
48. Nguyen, S; Rodney, S. Ruoff. Preparation and Characterization of Graphene Oxide Paper. *Nature* **2007**, *448*, 457–461.
49. Dan, L.; Marc, B. M.; Scott, G.; Richard, B. K.; Gordon, G. W. Processable Aqueous Dispersions of Graphene Nanosheets. *Nat. Nanotechnol.* **2007**, *3*, 101–105.